The EMBO Journal Vol.18 No.17 pp.4711–4721, 1999

Molecular determinants of glycine receptor subunit assembly

Nathalie Griffon[1,2], Cora Büttner[3], Annette Nicke[3], Jochen Kuhse[1,4], Günther Schmalzing[3] and Heinrich Betz[1,5]

[1]Department of Neurochemistry, Max-Planck-Institute for Brain Research, Deutschordenstrasse 46, D-60528 Frankfurt am Main and [3]Department of Pharmacology, Biocenter of the Johann Wolfgang Goethe-University, Marie-Curie-Strasse 9, D-60439 Frankfurt am Main, Germany

[2]Present address: Unité de Neurobiologie et Pharmacologie Moleculaire, INSERM U 109, Centre Paul Broca 2ter, rue d'Alesia, 75014 Paris, France
[4]Present address: Department of Anatomy and Cellular Neurobiology, University of Ulm, Albert-Einstein-Allee 11, D-89069 Ulm, Germany

[5]Corresponding author
e-mail: neurochemie@mpih-frankfurt.mpg.de

The inhibitory glycine receptor (GlyR) is a pentameric transmembrane protein composed of homologous α and β subunits. Single expression of α subunits generates functional homo-oligomeric GlyRs, whereas the β subunit requires a co-expressed α subunit to assemble into hetero-oligomeric channels of invariant stoichiometry ($\alpha_3\beta_2$). Here, we identified eight amino acid residues within the N-terminal region of the α1 subunit that are required for the formation of homo-oligomeric GlyR channels. We show that oligomerization and N-glycosylation of the α1 subunit are required for transit from the endoplasmic reticulum to the Golgi apparatus and later compartments, and that addition of simple carbohydrate side chains occurs prior to GlyR subunit assembly. Our data are consistent with both intersubunit surface and conformational differences determining the different assembly behaviour of GlyR α and β subunits.

Keywords: glycine receptor/N-glycosylation/oligomerization/subunit stoichiometry

Introduction

Neurotransmitter receptors of the ligand-gated ion channel (LGIC) superfamily I include nicotinic acetylcholine, $GABA_A$, serotonin ($5\text{-}HT_3$) and glycine receptors (Betz, 1990; Barnard, 1992). These receptors are hetero-oligomeric proteins composed of homologous subunits sharing an extended ligand-binding N-terminal domain and four transmembrane-spanning segments (M1–M4). Their assembly occurs in a multi-step process, which includes both folding reactions and post-translational modifications following polypeptide synthesis and insertion into the endoplasmic reticulum (ER) membrane (for reviews see Hall, 1992; Green and Millar, 1995). The process of LGIC assembly displays strict selectivity in that only certain combinations of subunits are oligomerized and targeted to the plasma membrane. Specific interactions must therefore exist between individual LGIC subunits to provide for their proper stoichiometry and nearest neighbour relationships within different pentameric receptor complexes.

The best characterized LGIC is the nicotinic acetylcholine receptor (nAChR) in vertebrate muscle and the analogous electric organ of the marine ray *Torpedo*. This membrane protein is composed of four distinct subunits with a stoichiometry of $\alpha_2\beta\gamma\delta$ (Hall and Sanes, 1993; Galzi and Changeux, 1995). Heterologous expression of combinations of cloned nAChR subunits followed by co-immunoprecipitation of the antagonist-tagged α subunit with antibodies specific for the β, γ or δ subunits allowed the identification of possible nAChR assembly intermediates (Blount *et al.*, 1990; Gu *et al.*, 1991a; Saedi *et al.*, 1991). Accordingly, the conformationally mature α subunit is thought to oligomerize with either the δ or γ subunits to form αδ and αγ heterodimers. These heterodimers then associate with the β subunit to form $\alpha_2\beta\gamma\delta$ complexes. An alternative model proposed from [^{35}S] methionine labelling experiments suggests that αβγ trimers recruit δ subunits into αβγδ to generate $\alpha_2\beta\gamma\delta$ pentamers by incorporation of a second copy of the α polypeptide (Green and Claudio, 1993).

Mutational analysis has identified sequence elements and amino acid residues within the extracellular domain of nAChR subunits that are critical for subunit interactions (Gu *et al.*, 1991b; Yu *et al.*, 1991; Chavez *et al.*, 1992; Verrall and Hall, 1992; Kreienkamp *et al.*, 1995; Sugiyama *et al.*, 1996). Similarly, the N-terminal domains of $GABA_A$ receptor subunits have been found to determine their assembly properties (Hackam *et al.*, 1997). This suggests that the extracellular regions of LGIC proteins are important for post-translational recognition between subunits. Presumably, this recognition occurs shortly after polypeptide synthesis, since only assembled pentameric nAChRs have been found to exit the ER and reach the cell surface; unassembled or misfolded subunits and partial assembly intermediates, in contrast, are retained and degraded intracellularly (Blount *et al.*, 1990; Gu *et al.*, 1991a; Chavez *et al.*, 1992). Also, $GABA_A$ receptor polypeptides appear at the cell surface only upon expression of defined subunit combinations, but otherwise remain in the ER (Conolly *et al.*, 1996; Gorrie *et al.*, 1997).

The inhibitory glycine receptor (GlyR) provides an ideal model system to study the molecular determinants of LGIC subunit assembly. The GlyR consists of only two types of glycosylated membrane-spanning polypeptides, the ligand-binding α and the structural β subunits of 48 and 58 kDa, respectively (Schmitt *et al.*, 1987; Betz, 1992). So far, four α (α1–α4) subunit genes and a unique β subunit gene of the GlyR have been identified (for a review see Kuhse *et al.*, 1995). Cross-linking experiments have shown that the native GlyR in adult spinal cord is

an $\alpha1_3\beta_2$ pentamer (Langosch *et al.*, 1988), whereas embryonic spinal cord is likely to contain $\alpha2_5$ homo-oligomeric receptors (Hoch *et al.*, 1989; Takahashi *et al.*, 1992). All GlyR α subunits assemble into functional homo-pentameric channels upon heterologous expression in *Xenopus* oocytes or mammalian cells (Schmieden *et al.*, 1989, 1992; Sontheimer *et al.*, 1989; Grenningloh *et al.*, 1990; Kuhse *et al.*, 1990a,b; Akagi *et al.*, 1991; R.J.Harvey, V.Schmeiden, A.von Holst, B.Laube, H.Rohrer and H.Betz, submitted). Furthermore, the α1 and α2 subunits have been shown to co-oligomerize at variable stoichiometries (Kuhse *et al.*, 1993). In contrast, the β subunit incorporates into functional GlyRs only upon co-expression with α subunits, resulting in an invariant $\alpha_3\beta_2$ heteromer composition. The GlyR thus is a LGIC protein that exists in both homo- and hetero-oligomeric forms.

Previous work from our laboratory has identified sequence motifs in the extracellular domains of GlyR subunits that determine their assembly behaviour and surface expression (Kuhse *et al.*, 1993). In particular, short regions of sequence divergence between the α and β subunits ('assembly boxes') were shown to govern GlyR subunit stoichiometry and to direct homo- versus hetero-oligomer formation. Here, we further examined the molecular basis of GlyR subunit assembly by combining electrophysiological, immunocytochemical and biochemical approaches to analyse the assembly behaviour of mutagenized subunits expressed in *Xenopus* oocytes and transiently transfected mammalian cells. Our results indicate that eight amino acid positions within the N-terminal region of the α1 subunit are critical for homo-oligomerization. Mutant GlyR subunits which do not form homo-oligomeric channels fail to exit the ER and are not complex-glycosylated unless they are assembled with other α subunits. Our findings are consistent with both intersubunit surface and conformational differences contributing to the different assembly behaviour of GlyR α and β subunits.

Results

Identification of residues important for homo-oligomer formation

We have shown previously that the invariant subunit stoichiometry of the adult $\alpha1_3\beta_2$ GlyR depends on short sequence motifs (assembly boxes) in the N-terminal half of the extracellular region of the β subunit (Kuhse *et al.*, 1993). The corresponding segments of the different α subunit isoforms in contrast promote homo-oligomerization as well as hetero-oligomer formation with other α subunits at variable subunit stoichiometries. The capacity to form either homo-oligomers or heteromeric GlyRs of defined subunit composition appears to be an exclusive property. A chimeric subunit (C4), composed of the N-terminal extracellullar region of the β subunit and the C-terminal membrane-spanning domain of the α1 subunit, does not assemble into homo-oligomeric GlyR channels but readily forms hetero-oligomers of defined stoichiometry with α subunits (Kuhse *et al.*, 1993). In other words, the C4 chimera behaves like a native β subunit. Notably, replacement of two or three of the four assembly boxes in the N-terminal β portion of the C4 chimera by the corresponding residues of the α1 sequence changes its stoichiometric assembly behaviour into an α1-like one. Formation of homo-oligomeric GlyRs is seen consistently with C4 substitutions which contain either boxes 1 and 3 (chimera C4D), or boxes 1, 2 and 8 (chimera C4B), respectively, of the α1 subunit (Figure 1A; see Kuhse *et al.*, 1993).

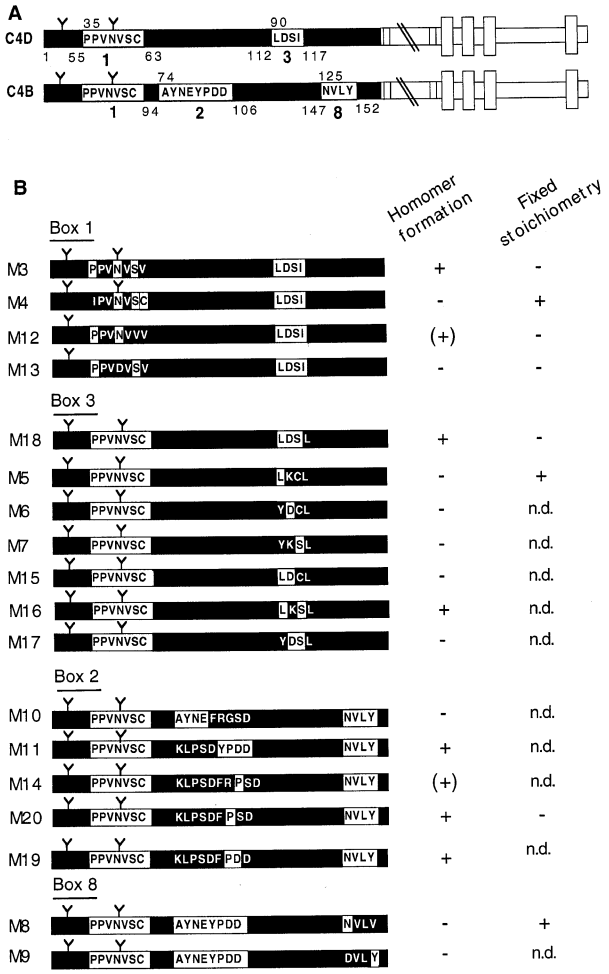

Fig. 1. Schematic representation of chimeric and mutant GlyR subunits. Sequences encoded by fragments of the α1 cDNA are indicated by white, and those representing β residues by black bars; hydrophobic stretches thought to be membrane-spanning regions (M1–M4) are symbolized by open intersecting rectangles. The positions of two extracellular cysteines characteristic of all LGIC class I proteins and of two cysteines found in all GlyR subunits are marked by line pairs. The positions of putative N-glycosylation sites are indicated by a Y. (**A**) Sequence boxes substituted in chimeras C4B and C4D. Boxes 1, 2, 3 and 8 show regions where the β coding sequence was converted into the corresponding nucleotides of the α1 cDNA (Kuhse *et al.*, 1993). Amino acid numbers corresponding to the β sequence are indicated below, and numbers corresponding to the α1 sequence, above the boxes. (**B**) Left: schematic representation of the β subunit-derived N-terminal regions of the C4B and C4D mutants. Substitutions in boxes 1, 3, 2 and 8 are indicated. Right: summary of the functional properties of the different mutants. The presence or absence of a glycine response in oocytes injected with RNAs synthesized on the respective templates is indicated by a '+' or a '–' under 'Homomer formation'. A + under 'Fixed stoichiometry' refers to an invariant subunit stoichiometry, as revealed by co-expression with the α1 or the $\alpha2^{G167L}$ subunits. All mutants shown in (B) co-assembled with the α1 or $\alpha2^{G167L}$ subunits into hetero-oligomeric GlyRs. n.d., not determined.

Combining site-directed mutagenesis and heterologous expression in *Xenopus* oocytes, we have now identified the minimal determinants responsible for homo-

oligomerization. To this end, we substituted single or multiple residues in the α1 sequence boxes of the C4D and C4B chimeras by the side chains found at the corresponding positions of the β subunit and determined whether the resulting mutants still formed functional homo-oligomeric receptor channels. In addition, we used co-expression with the native α1 subunit, or a low-affinity mutant of the α2 subunit, $\alpha2^{G167L}$ (Kuhse *et al.*, 1993), to reveal whether the mutated polypeptides assemble into hetero-oligomeric channels. This can be detected readily by corresponding shifts in the agonist dose–response profiles of the respective homomeric α1 or $\alpha2^{G167L}$ receptors. The subunit composition of heteromeric channels formed by mutants displaying an α-like assembly behaviour is variable and depends on the cRNA ratios injected, whereas β-like mutants generate channels of fixed subunit stoichiometry independently of the cRNA ratios injected (Kuhse *et al.*, 1993).

Replacement analysis of the box 1 region in chimera C4D showed that Asn38 and Ser40, which form a putative N-glycosylation site, as well as Pro35 but not Cys41 were required for homo-oligomer formation (mutant M3, see Figures 1B and 2A; Table I). Mutant M12 which only included Pro35 and Asn38 of the α1 subunit, also formed a functional GlyR, but at much lower efficiency as compared with the wild-type α1 subunit (Figure 2C). Both mutant M12 and mutant M13, which lacks Asn38 of the putative N-glycosylation consensus site (Figure 1B), generated hetero-oligomeric channels upon co-expression with the $\alpha2^{G167L}$ subunit; the subunit stoichiometries of these channels, however, varied with different ratios of the injected cRNAs (Figure 2C and D; Table I). In contrast, in mutant M4, replacement of Pro35 by isoleucine found at the homologous positions of the β subunit produced a β-like assembly behaviour, resulting in channels of invariant subunit stoichiometry upon co-expression with $\alpha2^{G167L}$ (Figure 2B; Table I).

Mutational analysis of box 3 in the C4D chimera indicated that the α1 residues Leu90 and Ser92 are necessary to generate a functional homo-oligomeric channel. A C4D chimera having both residues (M16) was gated by glycine concentrations similar to that activating the α1 wild-type GlyR (Figure 1B; Table I). All other C4D box 3-derived mutants, in which one of these two residues had been substituted by the corresponding β amino acids tyrosine and cysteine (mutants M6, M7, M15 and M17), failed to form functional homo-oligomers but co-assembled with the $\alpha2^{G167L}$ subunit (Figure 1B; Table I). Mutant M5, carrying only Leu90 but not Ser92, generated hetero-oligomeric channels whose subunit stoichiometries varied upon co-expression with different ratios of the $\alpha2^{G167L}$ cRNA (Table I). Thus, these box 3 residues constitute important determinants of α:β stoichiometry.

In the box 2 region, the sequences of the α1 and β subunits are highly divergent, and the β sequence contains an additional amino acid residue. Initial experiments with mutated C4B chimeras showed that the C-terminal residues of the α1 sequence of box 2 are required for the formation of homo-oligomeric GlyRs. Mutant M10, which included the N-terminal half of box 2 of the α1 subunit, did not form functional channels, whereas mutant M11 containing the C-terminal region of the α1 box 2 generated a GlyR whose low glycine affinity resembled that of the C4B chimera (Figure 1B; Table I). In fact, insertion of the α1 residue Pro79 into box 2 of the β subunit (mutant M14) proved sufficient to generate homo-oligomeric channels, albeit with low efficiency (not shown). In mutants M20, which included Pro79, and M19, which contained both Pro79 and Asp80 of the α1 subunit, the β residue Arg101 was deleted. Notably, all these mutants containing a box 2 region of the same length as the wild-type α1 polypeptide generated homo-oligomeric channels with current amplitudes comparable with that of the C4B chimera and were gated by lower concentrations of glycine than C4B (Figure 1B; Table I). The C4B chimera displays a significantly lower apparent glycine affinity (EC_{50} = 45.0 ± 9.0 mM) than both the wild-type α1 (EC_{50} = 0.26 ± 0.03 mM) and C4D (EC_{50} = 0.20 ± 0.04 mM) GlyRs, suggesting that boxes 2 and/or 8 may contribute to the formation of the agonist-binding site (Schmieden *et al.*, 1992, 1993). Also, all C4B box 2-derived mutants co-assembled with the α1 subunit (Table I), and mutant M20 generated hetero-oligomeric GlyRs of variable

Table I. Glycine dose–response properties of oocytes injected with different chimeric and mutant GlyR cRNAs

cRNAs injected	Ratio	EC_{50} (mM)	*h*	*n*
α1		0.26 ± 0.03	2.1 ± 0.3	6
$\alpha2^{G167L}$		26.27 ± 2.05	2.4 ± 0.2	4
C4D		0.20 ± 0.04	2.3 ± 0.3	3
M3		0.26 ± 0.02	2.0 ± 0.2	9
M3/$\alpha2^{G167L}$	5:1	1.38 ± 0.26	1.3 ± 0.3	3
	1:1	3.75 ± 0.07	1.2 ± 0.2	
	1:5	6.99 ± 1.05	1.2 ± 0.3	3
M4/$\alpha2^{G167L}$	5:1	8.69 ± 0.34	1.4 ± 0.2	3
	1:1	7.02 ± 0.48	1.5 ± 0.3	6
	1:5	8.33 ± 0.72	1.4 ± 0.4	3
M12		0.19 ± 0.02	1.9 ± 0.3	5
M12/$\alpha2^{G167L}$	5:1	2.62 ± 0.62	1.9 ± 0.3	4
	1:1	6.45 ± 0.32	1.3 ± 0.2	3
M13/$\alpha2^{G167L}$	5:1	2.41 ± 0.33	1.1 ± 0.2	4
	1:1	6.77 ± 0.67	1.4 ± 0.2	4
	1:5	16.26 ± 1.57	1.8 ± 0.3	3
M18		0.16 ± 0.05	2.1 ± 0.3	3
M5/$\alpha2^{G167L}$	1:1	9.04 ± 0.68	1.6 ± 0.3	6
	1:5	10.29 ± 0.95	1.8 ± 0.3	3
M6/$\alpha2^{G167L}$	1:1	8.95 ± 1.47	1.7 ± 0.2	3
M7/$\alpha2^{G167L}$	1:1	12.82 ± 1.17	1.5 ± 0.2	4
M15/$\alpha2^{G167L}$	1:1	3.04 ± 0.01	1.1 ± 0.1	3
M16		0.18 ± 0.03	1.7 ± 0.3	4
M16/$\alpha2^{G167L}$	1:1	10.30 + 3.20	2.3 ± 0.4	3
M17/$\alpha2^{G167L}$	1:1	4.48 ± 0.12	1.5 ± 0.2	3
C4B		45.06 ± 3.25	2.4 ± 0.4	5
M10/α1	1:1	13.75 ± 1.20	1.9 ± 0.3	5
M11		21.30 ± 2.70	1.6 ± 0.2	5
M11/α1	1:1	12.00 ± 2.18	2.0 ± 0.3	4
M14		10.10 ± 0.93	1.6 ± 0.3	2
M19		9.75 ± 1.17	1.7 ± 0.3	3
M20		22.42 + 5.40	1.8 ± 0.3	5
M20/α1	1:1	0.50 ± 0.09	2.5 ± 0.2	3
	5:1	12.20 ± 0.60	1.8 ± 0.4	4
M20/α2	1:1	26.77 ± 3.19	2.3 ± 0.2	2
M8/α1	1:1	0.37 ± 0.02	2.0 ± 0.3	3
M8/$\alpha2^{G167L}$	1:1	8.97 ± 1.20	1.8 ± 0.4	3
	5:1	8.87 ± 0.63	1.7 ± 0.3	4
M9/$\alpha2^{G167L}$	1:1	6.87 ± 1.09	1.7 ± 0.4	3

Oocytes were injected with individual cRNAs or the indicated ratios of two cRNAs, and glycine concentrations eliciting a half-maximal response (EC_{50}) were determined. Values represent the mean ± SEM of *n* determinations; *h*, Hill coefficient.

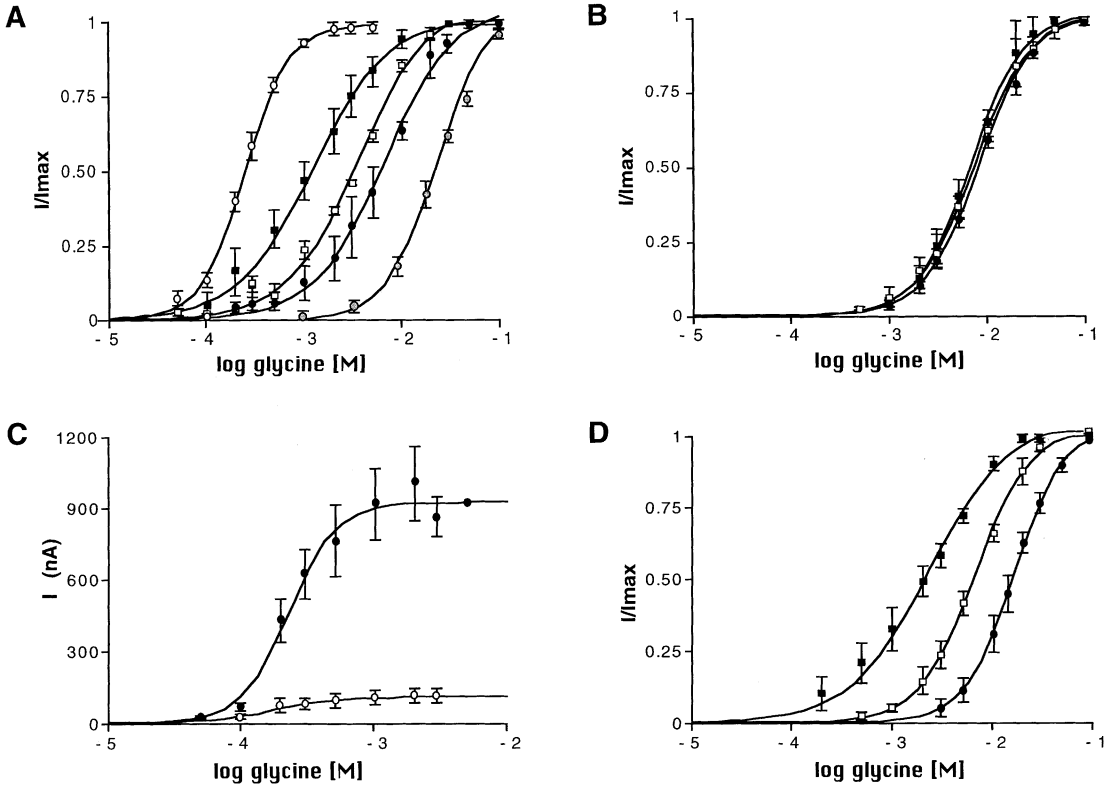

Fig. 2. Glycine dose–response curves of oocytes expressing box 1 mutant GlyRs. (**A**) Glycine dose–response curves obtained from oocytes injected with the mutant M3 cRNA alone (○, left), $\alpha2^{G167L}$ cRNA alone (○, right) or with both the M3 and the $\alpha2^{G167L}$ cRNAs at ratios of 5:1 (■), 1:1(□) and 1:5 (●). (**B**) As (A), but the oocytes were co-injected with the mutant M4 and the $\alpha2^{G167L}$ cRNAs at ratios of 5:1 (■), 1:1(□) and 1:5 (●). (**C**) Glycine dose–response obtained from oocytes injected with either the α1 (●) or the mutant M12 (○) cRNAs. (**D**) As (A), but oocytes were co-injected with the mutant M13 and the $\alpha2^{G167L}$ cRNAs at ratios of 5:1 (■), 1:1(□) and 1:5 (●), respectively.

stoichiometry when co-injected with different ratios of the α1 RNA (Table I). We therefore conclude that both Pro79 and the number of residues within the box 2 sequence are critical for efficient homo-oligomeric assembly.

In box 8, the residues Asn125 and Tyr128 are unique for α subunits. Both amino acids proved necessary for the formation of homo-oligomeric GlyRs, since replacement of Tyr128 in mutant M8 and of Asn125 in mutant M9 did not generate functional channels (Figure 1B). As M8 and M9 were derived from the low-affinity C4B chimera, we co-injected oocytes with the M8 and α1 cRNAs. The resulting channels were gated by glycine concentrations similar to that required at the wild-type α1 receptor; we therefore were unable to determine whether mutant M8 can co-assemble with the α1 polypeptide (Figure 3; Table I). However, after co-injection of mutant M8 with the $\alpha2^{G167L}$ cRNA, half-maximal currents were obtained with glycine concentrations that were significantly lower than for $\alpha2^{G167L}$ homo-oligomeric channels. As the dose–response curve of these hetero-oligomeric GlyRs proved to be independent of the cRNAs ratios injected, we conclude that mutant M8 has β-like assembly properties (Figure 3; Table I). Rather similar results were obtained for the M9 construct (Table I). Thus, the residues Asp148 and Val151, corresponding to Asn125 and Tyr128 of the α1 subunit, appear to be important determinants of an invariant GlyR subunit stoichiometry. Our results also suggest that substitution of Tyr128 by the respective β residue was responsible for the decrease in ligand-binding affinity observed with the C4B chimera.

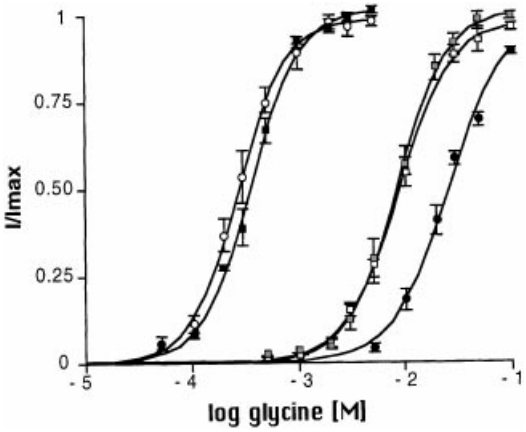

Fig. 3. Glycine dose–response curves of oocytes expressing a box 8 mutant GlyR. Glycine dose–responses were recorded from oocytes injected with either the α1 (○) or the $\alpha2^{G167L}$ (●) subunit cRNAs alone, or with mixtures of mutant M8 and either the α1 cRNA at a ratio of 1:1 (■) or the $\alpha2^{G167L}$ cRNA at ratios of 5:1 (▩) and 1:1(□), respectively.

In conclusion, our analysis identified eight amino acid residues within the assembly boxes of the N-terminal region of the α1 subunit that are critical for the formation of functional homo-oligomeric GlyR channels. In box 1, Asn38 and Ser40, which form a putative N-glycosylation site, as well as Pro35 were found to be essential for homo-oligomerization. In addition, Leu90 and Ser92 in box 3, Pro79 in box 2, and Asn125 and Tyr128 in box 8 of the

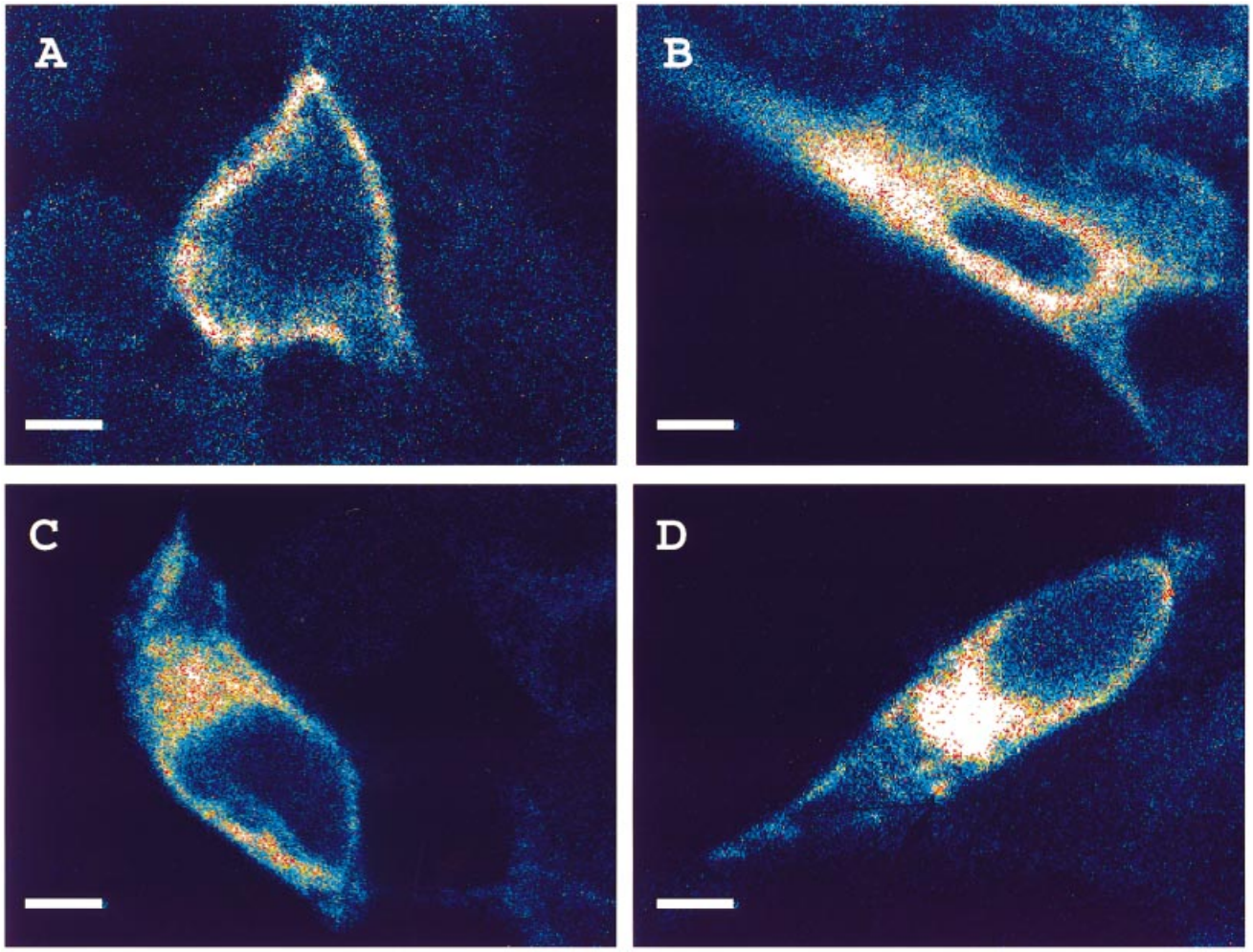

Fig. 4. Subcellular distribution of the box 1 mutant GlyRs in 293 cells. HEK 293 cells were transfected with cDNAs encoding different box 1 mutant subunits and immunostained as described in Materials and methods. The M3 mutant protein (**A**) was localized at the plasma membrane, whereas cells expressing the mutants M4 (**B**), M12 (**C**) and M13 (**D**) displayed strong intracellular labelling, consistent with a localization of these proteins in endomembranes. Bar, 5 μm.

C4B chimera were required for an α subunit-like assembly behaviour. Notably, both Pro35 and Pro79 are unique to the α1 subunit. As proline residues impose significant constraints on the secondary structures of proteins, conformational differences between the respective assembly boxes of GlyR α and β subunits could be crucial in determining their different assembly behaviour.

Plasma membrane targeting and oligomerization states of mutant GlyR subunits

In order to reveal whether substitutions affecting assembly behaviour might alter the processing and/or plasma membrane targeting of the resulting mutant GlyRs, we transfected mutants M3, M4, M12 and M13 engineered into a eukaryotic expression vector into human embryonic kidney (HEK) 293 cells and analysed the subcellular distribution of the recombinant proteins by immunostaining with a GlyR-specific monoclonal antibody, mAb 4a (Pfeiffer *et al.*, 1984). Confocal microscopy of the transfected cells revealed that mutant M3 was localized at the plasma membrane, as demonstrated by mAb 4a immunoreactivity lining the cell's circumference (Figure 4A). This distribution closely resembles that seen for the α1 subunit GlyR (Kirsch *et al.*, 1995). In contrast, in cells transfected with the mutants M4, M12 and M13, only intracellular labelling was observed (Figure 4B–D). These cells displayed a strong reticular immunostaining pattern reminiscent of ER labelling. Even in the case of mutant M12, which in *Xenopus* oocytes forms functional channels with low efficacy, no membrane labelling was detected (Figure 4C). This may reflect differences in expression efficiencies between oocytes and mammalian cells or, more likely, indicate that only a small percentage of the recombinant receptors reached the plasma membrane.

To demonstrate directly oligomer formation by wild-type and mutant GlyR subunits, we used affinity purification in combination with blue native polyacrylamide gel electrophoresis (Nicke *et al.*, 1998). First, wild-type and mutant subunits were hexahistidyl (His_6)-tagged at their C-terminal ends and expressed in *Xenopus* oocytes. Electrophysiological recording showed that the functional properties and the assembly behaviour of the α1 subunit and mutants M3, M4 and M13 were not affected by the His_6 tag (data not shown). To visualize solely GlyRs incorporated into the plasma membrane, we radioiodinated the outer cell surface of oocytes with [^{125}I]sulfosuccinimidyl-3-(4-hydroxyphenyl)propionate, a lysine-reactive membrane-impermeant com-

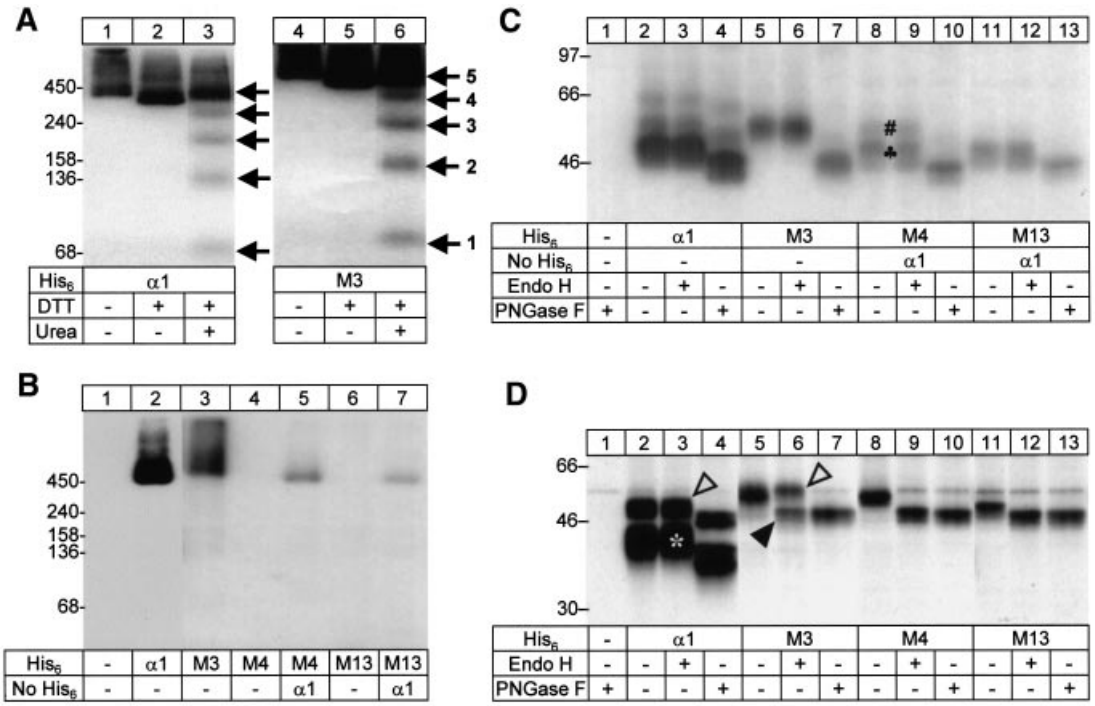

Fig. 5. Cell surface wild-type and mutant GlyRs are pentameric and complex-glycosylated. Oocytes injected with the indicated cRNA(s) were surface-labelled with [^{125}I]sulfo-SHPP. The α1-His$_6$ and the different His$_6$-tagged box 1 mutant proteins were then purified under non-denaturating conditions, resolved by PAGE and visualized by autoradiography. (**A**) Blue native PAGE analysis (4–13% acrylamide gradient gel) of α1-His$_6$ (α1) and M3-His$_6$ (M3) either without further treatment of after incubation with 0.1 M DTT and 8 M urea as indicated. Numbered arrows indicate the positions of monomers, dimers, trimers, tetramers and pentamers. (**B**) Blue native PAGE analysis (4–10% acrylamide gradient gel) of all His$_6$ constructs immediately after native elution. Iodinated M3 and M13 polypeptides are found only upon co-expression of the untagged α1 subunit. (**C**) Aliquots of the radiolabelled samples shown in (B) were incubated for 2 h at 37°C with SDS sample buffer and 20 mM DTT in the absence or presence of Endo H or PNGase F, prior to SDS–PAGE and autoradiography. Note that the M3 polypeptide carries two N-glycans, as indicated by a larger mobility shift (~6 kDa), whereas α1 and M13 have only one N-glycan substitution, and that all N-glycans are in Endo H-resistant form. The doublet (#, ♣) visible in lanes 8 and 9 results from co-isolation of non-tagged α1-His$_6$ with M4-His$_6$, which carry one and two N-glycans, respectively. No such doublet is found in lanes 11 and 12, since M13-His$_6$ possesses only one N-glycan and hence migrates at approximately the same position as α1-His$_6$. (**D**) SDS–PAGE analysis of all His$_6$ constructs isolated after a 6 h pulse of [^{35}S]methionine labelling and a subsequent 40 h chase period. Samples were prepared as in (B). Open arrows, Endo H-resistant polypeptides; filled arrow, Endo H-sensitive form of M3-His$_6$ that is not observed at the plasma membrane (C); asterisk, EndoH-resistant 40 kDa degradation product of α1-His$_6$ that is also not seen upon surface labelling (C).

pound (Thompson *et al.*, 1987). GlyR polypeptides were then isolated by Ni^{2+}-NTA chromatography under non-denaturing conditions from digitonin extracts of these oocytes. When resolved by blue native PAGE and visualized by autoradiography, surface GlyR formed from α1-His$_6$ or M3-His$_6$, exhibited a mobility corresponding to that of soluble marker proteins of an apparent molecular mass of ~350 kDa (Figure 5A; lane 1) or 400 kDa (Figure 5A, lane 4), respectively. These masses are consistent with oligomers, but larger than the 270 kDa expected for a glycosylated pentameric GlyR (Pfeiffer *et al.*, 1982; Langosch *et al.*, 1988). Since blue native PAGE is a charge shift method (Schägger *et al.*, 1994), a likely explanation is that the excess of negative charges conferred to the analysed protein by bound Coomassie Blue G dye did not suffice to render the electrophoretic mobility of GlyR-His$_6$ entirely independent of its intrinsic basic charges (Nicke *et al.*, 1998).

To determine the number of subunits in the purified complex by an approach that is independent of Coomassie and detergent binding and intrinsic charges, we elaborated conditions that induce partial dissociation of the GlyR. Incubation prior to blue native PAGE of the natively eluted α1-His$_6$ receptor with the strong reductant dithiothreitol (DTT) in the presence of sodium 6-amino-*n*-caproate (Figure 5A, lane 2) had no significant effect, but combined treatment with 0.1 M DTT and 8 M urea induced the appearance of four additional protein bands besides the 350 kDa GlyR complex (lane 3). These bands of apparent masses of ~70, 140, 210 and 280 kDa correspond to α1-His$_6$ monomers, dimers, trimers and tetramers, respectively, indicating that the non-denatured 350 kDa protein band must be a pentamer. Similar results were obtained when dodecyl-β-D-maltoside instead of digitonin was used as detergent (data not shown). Furthermore, dissociation of the 400 kDa M3-His$_6$ complex with DTT and urea produced an identical pattern of lower order oligomers (Figure 5A, lanes 5 and 6). These results corroborate previous cross-linking (Langosch *et al.*, 1988) and electrophysiological (Kuhse *et al.*, 1993) data, which indicate a pentameric structure of the GlyR.

In contrast to the observations made with the α1-His$_6$ and M3-His$_6$ polypeptides, no ^{125}I-labelled protein could be isolated from surface-iodinated oocytes expressing mutants M4-His$_6$ (Figure 5B, lane 4) and M13-His$_6$ (Figure 5B, lane 6). Apparently, these mutant subunits were not inserted into the plasma membrane. Upon co-expression with non-tagged α1 subunit, however, complexes similar to the pentameric α1-His$_6$ GlyR could be observed in native blue PAGE (Figure 5B, lanes 5 and 7).

We therefore conclude that mutants M4-His_6 and M13-His_6 require co-assembly with the wild-type α1 subunit for transport to and/or incorporation into the plasma membrane.

SDS–PAGE analysis of the ^{125}I-labelled GlyR complexes yielded apparent masses of 48 and 51 kDa for the monomeric forms of α1-His_6 and M3-His_6, respectively (Figure 5C, lanes 2 and 5). The 3 kDa larger mass of M3-His_6 reflects a difference in the number of N-glycans, since the α1 sequence harbours a single consensus N-glycosylation site in the box 1 region of its N-terminal sequence, whereas mutant M3 has two such sites (Figure 1B). The first is located in the N-terminal β portion of the chimera, and the second in the α1-derived box 1. Indeed, upon removal of N-glycans by treatment with peptide:N-glycosidase F (PNGase F), both the α1-His_6 and M3-His_6 polypeptides migrated at ~45 kDa, consistent with the removal of one and two N-glycans of 3 kDa, respectively (Figure 5C, lanes 4 and 7). Treatment with endoglycosidase H (Endo H) failed to alter the mobility of α1-His_6 and M3-His_6 (Figure 5C, lanes 3 and 6), indicating that the N-glycans of both proteins were in the complex-glycosylated form. Thus, apparently both proteins were able to exit the ER and reach the Golgi apparatus prior to incorporation into the plasma membrane. In contrast, under the same conditions, mutants M4-His_6 and M13-His_6 carried Endo H-resistant carbohydrates only upon co-expression with the non-tagged α1 subunit (Figure 5C, lanes 8–13); this is consistent with their targeting to the plasma membrane requiring hetero-oligomerization. Collectively these data suggest that oligomer formation is a prerequisite for transit from the ER to the Golgi apparatus and later compartments, such as the plasma membrane.

To allow for the visualization of the singly expressed mutants M4 and M13 that were not transported to the plasma membrane, we metabolically labelled newly synthesized proteins in cRNA-injected oocytes with [^{35}S] methionine. Figure 5D shows that the M3, M4 and M13 polypeptides were present in similar amounts in *Xenopus* oocytes after a 40 h chase period, indicating that all three chimeras were synthesized efficiently and were metabolically stable. Since only a minor fraction of α1-His_6 and ⩽50% of M3-His_6 isolated from [^{35}S]methionine-labelled oocytes was sensitive to Endo H treatment (Figure 5D, lanes 3 and 6), apparently a major fraction of both proteins was able to exit the ER and reach the Golgi apparatus and later compartments, such as the plasma membrane. In contrast, mutants M4-His_6 and M13-His_6 did not acquire Endo H-resistant carbohydrates (Figure 5D, lanes 9 and 12), corroborating the view that these mutant subunits were retained in the ER. Notably, a major fraction of α1-His_6 was isolated as a 40 kDa degradation product that was apparently formed after endocytotic retrieval of the receptor from the plasma membrane, since the 40 kDa band was observed neither directly after the pulse nor at the plasma membrane (Figure 5C).

Discussion

The results presented in this study show that the different assembly properties of GlyR α and β subunits are determined by defined amino acid substitutions in the highly conserved N-terminal regions of these polypeptides. These substitutions lie within the previously identified 'assembly boxes', i.e. short stretches of sequence divergence between the α and β subunits, which have been shown to define homo- versus hetero-oligomeric assembly behaviour (Kuhse *et al.*, 1993). In the α1 subunit, two different combinations of these boxes are known to result in the same assembly phenotype. Box 1 has to combine with either box 3 or, alternatively, with boxes 2 and 8 to result in homo-oligomerization. Here, single and multiple amino acid substitutions in the chimeric subunits C4B and C4D revealed that in box 1 three out of four (Pro35, Asn38 and Ser40), in box 3 two out of four (Leu90 and Ser92), and in box 8 two out of two (Asn125 and Tyr128) divergent residues had to be from the α1 sequence to produce homo-oligomeric GlyRs (Figure 6A). However, in box 2, which represents the most divergent sequence region between α and β subunits, only a single amino acid residue, Pro79, proved critical for the α1-like assembly phenotype. In addition, the divergent lengths of this box in the α and β subunits apparently contribute to their different assembly behaviour. We therefore conclude that at least eight distinct residues determine the different assembly properties of GlyR α and β subunits.

Putative locations of assembly determinants

Recently, Gready *et al.* (1997) have proposed structural models for the monomeric and pentameric forms of the extracellular region of the GlyR α1 subunit by using an inverted protein structure prediction approach based on similarities between GlyR subunits and the SH2–SH3 domains of the biotin repressor. Residues involved in intersubunit contacts were located by comparing solvent accessibility values in both the mono- and the pentamer. Accordingly, the first part of the N-terminal extracellular region of the α1 subunit is homologous to the SH2 domain. Pro35 is predicted to be located in a loop of the extracellular domain, and residues Asn38 and Ser40 in a peripheral β sheet, with Asn38 being close to the top of the folded polypeptide (Figure 6B). The two crucial residues in box 3, Leu90 and Ser92, would be located peripherally but not at the subunit interface, and Pro79 would lie in a region corresponding to the main immunogenic region of the nAChR, suggesting surface exposure of this amino acid (Beroukim and Unwin, 1995; Gready *et al.*, 1997). Residues Asn125 and Tyr128 are predicted to be at the subunit interface and thus in direct contact with the neighbouring subunit.

A model for the nAChR extracellular domain based on sequence identities with copper-binding proteins (Tsigelny *et al.*, 1997) also suggests amino acids Asn125 and Tyr128 to be at the subunit interface. Figure 6C shows the predicted positions of the amino acid residues of the nAChR α1 subunit that are homologous to the GlyR α1 subunit residues involved in homo-oligomer formation. The resulting locations of residues in boxes 1 and 8 are similar to those emerging from the model of Gready *et al.* (1997). Pro69 of the nAChR α1 subunit (homologous to Pro79 of the GlyR α1 subunit) is found at the lumenal side close to the subunit interface, opposite to residues in box 8. Again, residues in boxes 2 and 3 are found to be close to each other, but the side chains of Leu80 and Ser82 (homologous to Leu90 and Ser92) are now predicted

to be buried within the protein's core region. In conclusion, these predictions from protein modelling suggest that Asn125 and Tyr128 may be exposed at subunit interfaces and regulate assembly by mediating protein–protein interactions.

Both models shown in Figure 6 propose positions for Asn38 and Ser40 that are consistent with N-glycosylation events, as confirmed by our biochemical data. Pro35 and Pro79, located in loops or turns, might be important in determining the secondary structure of the polypeptide and its higher order conformation. In addition, these residues may confer conformational flexibility required during the formation of intersubunit contacts. The predicted position of box 3 residues is consistent with these amino acids not being involved directly in the assembly process. Their proximity to box 2 also suggests that the presence of either Pro79 or Leu90 and Ser92 in chimeras C4B or C4D, respectively, stabilizes a structure favouring homo-oligomerization. The different assembly behaviour of α and β subunits thus might be related to subtle differences in the tertiary structures of these highly homologous subunits.

Mutational studies have led to a three loop model of the ligand pocket of class I LGICs where agonist binding involves multiple interactions with at least three different domains within the extracellular region of the α subunits. The currently available data indicate a rather similar structure of the ligand-binding site for GlyRs, nAChRs and $GABA_A$ receptors (Devillers-Thiéry *et al.*, 1993). In contrast, both homologous positions in the extracellular domains of the receptor polypeptides and regions diverging considerably between different receptor subunits have been implicated in LGIC assembly. In the case of the nAChR, Cys106 and Ser115 of the ε subunit and amino acids 105–120 of the β subunit have been shown to be important for receptor assembly (Gu *et al.*, 1991b; Kreienkamp *et al.*, 1995). From multiple sequence alignment, the corresponding GlyR residues lie within box 8 which we suggest to be located at the subunit interface. However, Lys145 and Lys150 of the δ subunit and Ile145 and Thr150 of the γ subunit, i.e. residues known to be involved in the assembly with the α subunit and the

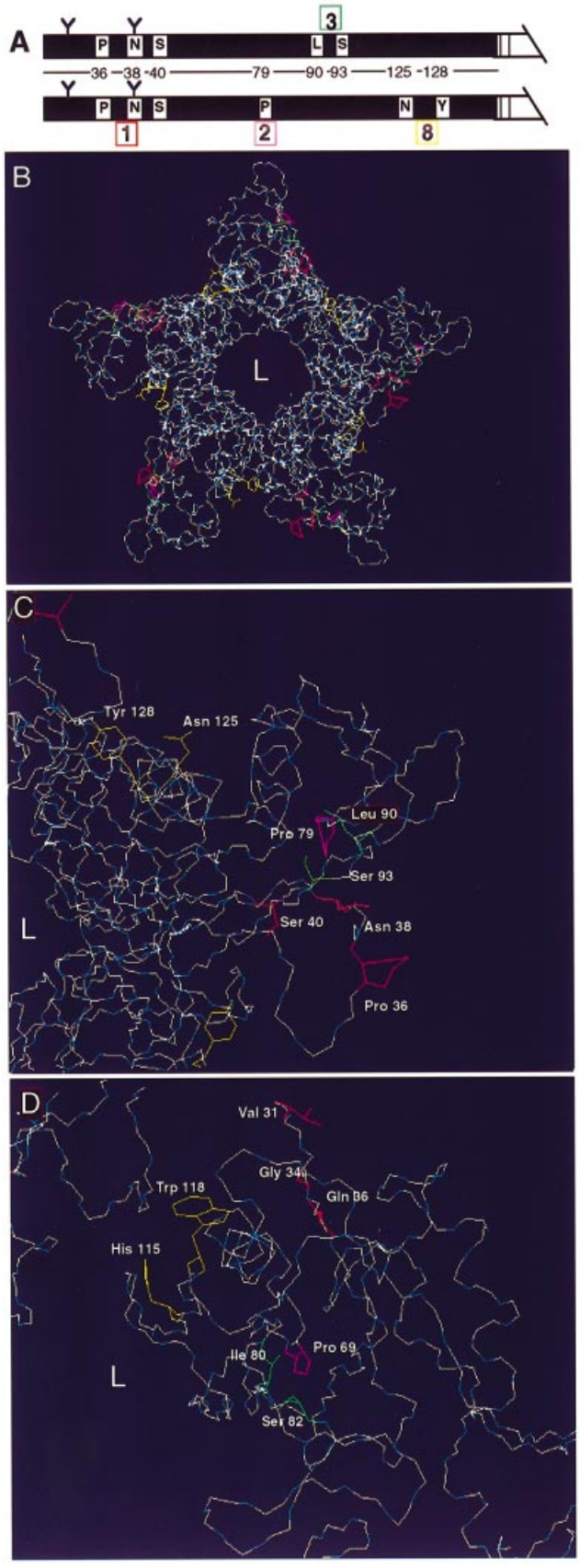

Fig. 6. Putative locations of amino acid residues determining the assembly behaviour of GlyR subunits. (**A**) Schematic drawing of the extracellular region of the GlyR α1 subunit; amino acid positions important for its assembly behaviour are indicated. The two combinations of assembly boxes allowing homo-oligomerization are shown; the colouring of amino acid residues is as in (B–D). Putative N-glycosylation sites are indicated by a Y. (**B**) Top view of the pentameric α1 GlyR as modelled by Gready *et al.* (1997). The central ion channel formed by the pentameric arrangement of subunits is indicated by an L (for lumen). Residues of the different assembly boxes are indicated in red for box 1, pink for box 2, green for box 3 and yellow for box 8, respectively. (**C**) Enlargement of (B). Two residues of box 8 (yellow) as well as the proline residue (P79; pink) that constitutes a particular important determinant of assembly box 2, are indicated. Note that Tyr128 in one of three predicted α-helical segments of the α1 subunit is in direct contact with the neighbouring subunit. (**D**) For comparison, a structural model of the N-terminal domain of the nAChR α1 subunit based on homology to the copper-binding proteins plastocyanin and pseudo-azurin is shown (Tsigelny *et al.*, 1997). In a top view of the α1-binding domain with its interfaces to neighbouring subunits, the amino acid positions homologous to the GlyR α1 subunit residues depicted in (A) are indicated. Residues V31, G34 and Q36 correspond to residues in the assembly box 1 of the GlyR α1 subunit, P69 is homologous to P79 of the α1 subunit, I80 and S82 can be aligned with residues L90 and S93, and H115 and W118 are homologous to N125 and Y128, respectively. Note that as in (C), residues of box 8 are facing the neighbouring subunits.

formation of higher order oligomers, are not located at positions homologous to the GlyR assembly boxes identified here. Furthermore, in the case of the nAChR, amino acids adjacent or identical to side chains that form the ligand-binding site have been found to contribute to the specificity of subunit assembly, e.g. Tyr117 in the γ subunit, and Ser187 and Thr189 in the α subunit (Claudio, 1989; Fu and Sine, 1994). This is in contrast to our findings for the GlyR where substitutions which affect channel activation by agonist or blockade by antagonists (amino acids 159, 160, 161, 200, 202 and 204 of the α1 subunit; see Kuhse *et al.*, 1995) are clearly distant from those determining the assembly behaviour of α and β subunits.

Subunit assembly as a prerequisite for ER exit

Our results also shed light on post-oligomerization steps of GlyR biosynthesis including N-glycosylation and subsequent exit from the ER. The α1 subunit of the GlyR has one consensus site for N-glycosylation located at Asn38, whereas the β subunit harbours two potential N-glycosylation sites at positions Asn33 and Asn220. All GlyR chimeras used here carry the first N-glycosylation consensus site of the β subunit; in addition, most of our mutants included the consensus site derived from the α1 subunit sequence (Figure 1B). Consistent with the use of both predicted N-glycosylation motifs, the M3 mutant harbouring both sites displayed a higher apparent molecular mass upon SDS–PAGE than the α1 subunit, whereas both polypeptides migrated similarly after removal of N-glycans by PGNase F. As N-glycosylation of the M3 chimera at Asn38 did not prevent homo-oligomerization and targeting to the plasma membrane, the different assembly behaviour of GlyR α and β subunits cannot be attributed to differences in the number of N-glycan side chains.

Electrophysiological recording, immunocytochemistry and cell surface iodination revealed that GlyR α1 homopentamers were transported efficiently out of the ER. As apparent from the quantitative acquisition of Endo H-resistant complex-type carbohydrates, only the fully mature glycoprotein appeared at the plasma membrane. Likewise, mutant M3 also was able to assemble into a homopentamer, to acquire complex-type carbohydrates and to reach the plasma membrane in the fully mature form carrying two complex-type N-glycans. In contrast, the box 1 mutants M4 and M13 were not incorporated into the plasma membrane, but retained in the ER. The apparent molecular mass of the M13 polypeptide mutated at Asn38 changed upon Endo H treatment, suggesting that N-glycosylation of the α1 subunit at this position is crucial for exit from the ER to the Golgi and later compartments, and cannot be overcome by glycosylation at the Asn33 site of the chimera. Similarly, glycosylated M4 monomers were sensitive to the enzyme. Notably, upon co-expression of the M4 and M13 mutants with the α1 subunit, complex N-glycosylation and surface expression of the resulting hetero-oligomers were seen. This is consistent with incorrect folding and/or a lack of post-translational modifications preventing these mutant polypeptides from assembling and exiting the ER to undergo the secondary glycosylation reactions that occur during the transport of glycoproteins through the Golgi apparatus. Apparently, the protein secretion machinery of the ER exerts a stringent quality control. Collectively, our results suggest that N-glycosylation at Asn38 of the α1 subunit is necessary for exit from the ER, and that the addition of simple carbohydrate side chains occurs before subunit assembly. In contrast, complex N-glycosylation was seen only with assembled subunits. We therefore conclude that assembly is a prerequisite for ER exit.

Similar findings have been reported for the nAChR α subunit, which also carries a conserved N-glycosylation site that has been found to be indispensable for the proper assembly and stability of the receptor complex (Blount and Merlie, 1990; Gehle and Sumikawa, 1991). Rickert and Imperiali (1995) have suggested that this complex N-glycan side chain may influence the local conformation of the receptor subunit. Importantly, the N-glycosylation site of the nAChR polypeptide is located within the so-called Cys–Cys loop which lies ~100 amino acid residues C-terminal from the N-glycosylation site in the GlyR α1 subunit. It therefore seems unlikely that these N-glycans are directly involved in a physical association of the receptor subunits by some type of lectin–carbohydrate interaction, although glycoprotein oligosaccharides have been found to serve in protein–protein interactions (for a review see Dwek, 1995). In our view, a role for the α1 subunit N-glycan in the quality control of newly synthesized proteins by the secretory pathway (Hebert *et al.*, 1995) appears more likely. This is consistent with preliminary observations demonstrating that GlyR α1 subunits synthesized without N-glycan in tunicamycin-treated oocytes assemble into pentamers, but are degraded rapidly (C.Büttner and G.Schmalzing, unpublished). We therefore suggest that the N-glycan at position 38 is needed to prevent the receptor from entering a degradation pathway before leaving the ER.

In conclusion, the data presented herein point to a complex coding of GlyR subunit assembly properties. We previously have proposed that the different assembly boxes of the α and β subunits allowing either homo-oligomeric channel formation or stoichiometric assembly, respectively, may be crucial for achieving a sequential assembly pathway of the heteromeric GlyRs expressed *in vivo* (Kuhse *et al.*, 1993). In particular, determinants within assembly boxes 3 and 8 were postulated to be exposed at subunit interfaces and to regulate receptor assembly by hydrophobic protein–protein interactions. From the data presented here, only box 8 residues are likely to have such a direct role in intersubunit contact. The other assembly determinants identified here may regulate conformational features that could be essential for substeps of the assembly reaction in the ER. Attempts to identify the latter are in progress in our laboratory.

Materials and methods

Site-directed mutagenesis

Site-directed mutagenesis was performed using the QuickChange™ site-directed mutagenesis kit (Qiagen). As templates, the cDNAs of the chimeric subunits C4B and C4D, subcloned in the BlueScript KS vector (Stratagene), were used. In these chimeras, the cDNA fragments encoding amino acids 1–153 of the β subunit are joined to the 3′-coding region of the α1 cDNA (Kuhse *et al.*, 1993). Substitutions in boxes 1, 2, 3 and 8 were introduced by replacing the respective amino acid codons of the β cDNA by the corresponding codons of the α1 subunit. For protein purification, a His_6 epitope was introduced by PCR-based mutagenesis

at the 3′ end of the coding region of the α1 as well as the chimeric and mutant subunits and subcloned into the pNKS2# vector (Gloor *et al.*, 1995). All constructs were verified by dideoxy sequencing of the entire coding sequence.

cRNA synthesis and oocyte expression

Linearized plasmid DNAs were used for *in vitro* synthesis of cRNA (mCAP™ mRNA capping kit, Stratagene). cRNAs of C4 chimeras and mutants were synthesized using T7 RNA polymerase, and the α1 and $\alpha2^{G167L}$ cRNAs using T3 RNA polymerase. cRNA concentrations were determined by both measuring the optical density at 260 nm and comparing ethidium bromide staining intensities after gel electrophoresis of cRNAs. For oocyte injection, the concentration of cRNA samples was adjusted to 50–500 ng/ml. For co-injection experiments, appropriatly diluted aliquots of the different cRNAs were mixed before injection to achieve the desired RNA ratios. One to 3 days after microinjection of ~50 nl of cRNA into *Xenopus* oocytes, glycine current responses were measured by two electrode-voltage clamp recording at a holding potential of –70 mV as described previously (Schmieden *et al.*, 1989).

Expression in mammalian cells and confocal microscopy

For subcellular distribution studies, HEK 293 cells (ATCC #CRC 1573) were transiently transfected using the Superfect™ transfection reagent (Qiagen) with cDNAS of GlyR mutants subcloned into the mammalian expression vector pBK/CMV (Stratagene). After 2 days, immunolabelling of the transfected cells under permeabilizing conditions was performed using the GlyR-specific antibody mAb 4a (Pfeiffer *et al.*, 1984) and Cy3-conjugated goat anti-mouse IgG (Dianova) as described (Kirsch and Betz, 1995). Immunoreactivities were visualized using a confocal laser scanning microscope (Molecular Dynamics).

Radioactive labelling of oocytes and protein purification

For selective labelling of plasma membrane GlyR, cRNA-injected oocytes and non-injected controls were incubated 3 days after injection with [^{125}I]sulfosuccinimidyl-3-(4-hydroxyphenyl)proprionate ([^{125}I]sulfo-SHPP), a membrane-impermeant derivative of the Bolton–Hunter reagent (Thompson *et al.*, 1987), exactly as described (Nicke *et al.*, 1998). His_6-tagged GlyR wild-type, chimeric and mutant subunits were then purified by Ni^{2+}-NTA–agarose (Qiagen) chromatography from digitonin (1% w/v) extracts of oocytes as detailed previously (Nicke *et al.*, 1998). Bound protein was released from the Ni^{2+}-NTA–agarose with non-denaturing elution buffer consisting of 1% (w/v) digitonin in either 20 mM Tris–HCl, 100 mM imidazole–HCl, 10 mM EDTA pH 7.8 or 250 mM imidazole–HCl pH 7.0, as indicated. Eluted proteins were kept at 0°C until analysed by PAGE. In some of the experiments, cRNA-injected oocytes and non-injected controls were metabolically labelled by the injection of oocytes with L-[^{35}S]methionine (>40 TBq/mmol, Amersham) at ~100 MBq/ml (0.4 MBq per oocyte) followed by incubation at 19°C for 6 h. Thereafter, the oocytes were subjected to a chase period of 40 h in 10 mM unlabelled methionine (Nicke *et al.*, 1998).

Blue native PAGE and SDS–PAGE

Blue native PAGE (Schägger and von Jagow, 1991; Schägger *et al.*, 1994) was performed as described (Nicke *et al.*, 1998). Before loading, purified proteins were supplemented with Blue native sample buffer to final concentrations of 10% (v/v) glycerol, 0.2% (w/v) Serva Blue G and 20 mM sodium 6-amino-*n*-caproate, and applied onto polyacrylamide gradient slab gels. Molecular mass markers (Combithek II, Boehringer Mannheim) were visualized by Coomassie staining. For SDS–PAGE, proteins were supplemented with SDS sample buffer containing DTT and electrophoresed in parallel with ^{14}C-labelled molecular mass markers (Rainbow, Amersham) on SDS–polyacrylamide gradient gels. Where indicated, samples were treated prior to SDS–PAGE with either Endo H or PNGase F (New England Biolabs) in the presence of 1% (w/v) octylglucoside to reduce inactivation of PNGase F. Gels were fixed, dried and exposed to BioMax MR or MS film (Kodak) at –80°C.

Acknowledgements

We thank Drs V.Schmieden and J.Kirsch for helpful advice on electrophysiological and confocal microscopy techniques. This work was supported by Deutsche Forschungsgemeinschaft (SFB 474), Fonds der Chemischen Industrie and a BIOMED 2 contract (BMH4-CT-97-2374).

References

Akagi,H., Hirai,K. and Hishinuma,F. (1991) Cloning of a glycine receptor subtype expressed in rat brain and spinal cord during a specific period of neuronal development. *FEBS Lett.*, **281**, 160–166.

Barnard,E.A. (1992) Receptor classes and the transmitter-gated ion channels. *Trends Biochem. Sci.*, **17**, 368–374.

Beroukhim,R. and Unwin,N. (1995) Three-dimensional location of the main immunogenic region of the acetylcholine receptor. *Neuron*, **15**, 1–20.

Betz,H. (1990) Ligand-gated ion channels in the brain: the amino acid receptor family. *Neuron*, **5**, 383–392.

Betz,H. (1992) Structure and function of inhibitory glycine receptors. *Q. Rev. Biophys.*, **25**, 381–394.

Blount,P. and Merlie,J.P. (1990) Mutational analysis of muscle nicotinic acetylcholine receptor subunit assembly. *J. Cell Biol.*, **111**, 2613–2622.

Blount,P., Smith,M.M. and Merlie,J.P. (1990) Assembly intermediates of the mouse muscle nicotinic acetylcholine receptor in stably transfected fibroblasts. *J. Cell Biol.*, **111**, 2601–2611.

Chavez,R.A., Maloo,J., Beeson,D., Newsom-Davis,J. and Hall,Z.W. (1992) Subunit folding and αδ heterodimer formation in the assembly of the nicotinic acetylcholine receptor. *J. Biol. Chem.*, **267**, 23028–23034.

Claudio,T. (1989) Molecular genetics of acetylcholine receptor-channels. In Glover,D.M. and Hames,B.D. (eds), *Frontiers in Molecular Biology* (*Molecular Neurobiology*). IRL Press Oxford, pp. 63–142.

Connolly,C.N., Krishek,B.J., McDonald,B.J., Smart,T.G. and Moss,S.J. (1996) Assembly and cell surface expression of heteromeric and homomeric γ-aminobutyric acid type A receptors. *J. Biol. Chem.*, **271**, 89–96.

Devilliers-Thiery,A., Galzi,J.L., Eisele,J.L., Bertrand,S., Bertrand,D. and Changeux,J.P. (1993) Functional architecture of the nicotinic acetylcholine receptor: a prototype of ligand-gated ion channels. *J. Membr. Biol.*, **136**, 97–112.

Dwek,R.A. (1995) Glycobiology: towards understanding the function of sugars. *Biochem. Soc. Trans.*, **23**, 1–25.

Fu,D.X. and Sine,S.M. (1994) Competitive antagonists bridge the α–γ subunit interface of the actylcholine receptor through quaternary ammonium–aromatic interactions. *J. Biol. Chem.*, **269**, 26152–26157.

Galzi,J.L. and Changeux,J.P. (1995) Neuronal nicotinic receptors: molecular organization and regulations. *Neuropharmacology*, **34**, 563–582.

Gehle,V.M. and Sumikawa,K. (1991) Site-directed mutagenesis of the conserved *N*-glycosylation site on the nicotinic acetylcholine-receptor subunits. *Mol. Brain Res.*, **11**, 17–25.

Gloor,S., Pongs,O. and Schmalzing G. (1995) A vector for the synthesis of cRNAs encoding Myc epitope-tagged proteins in *Xenopus laevis* oocytes. *Gene*, **160**, 213–217.

Gorrie,G.H., Vallis,Y., Stephenson,A., Whitfield,J., Browning,B., Smart,T.G. and Moss,S.J. (1997) Assembly of $GABA_A$ receptors composed of α1 and β2 subunits in both cultured neurons and fibroblasts. *J. Neurosci.*, **17**, 6587–6596.

Gready,J.E., Ranganathan,S., Schofield P.R., Matsuo,Y. and Nishikawa,K. (1997) Predicted structure of the extracellular region of ligand-gated ion-channel receptors shows SH2-like and SH3-like domains forming the ligand-binding site. *Protein Sci.*, **6**, 983–998.

Green,W.N. and Claudio,T. (1993) Acetylcholine receptor assembly: subunit folding and oligomerization occur sequentially. *Cell*, **74**, 57–69.

Green,W.N. and Millar,N.S. (1995) Ion-channel assembly. *Trends Neurosci.*, **18**, 280–287.

Grenningloh,G., Kuhse,J., Schofield,P.R., Seeburg,P.H., Siddique,T., Mohandas,T.K., Becker,C.M. and Betz,H. (1990) Alpha subunits variants of the human glycine receptor: primary structures, functional expression and chromosomal localization of the corresponding genes. *EMBO J.*, **9**, 771–776.

Gu,Y., Forsayeth,J.R., Verrall,S., Yu,X.M. and Hall,Z.W. (1991a) Assembly of the mammalian muscle acetylcholine receptor in transfected COS cells. *J. Cell Biol.*, **114**, 799–807.

Gu,Y., Camacho,P., Gardner,P. and Hall,Z.W. (1991b) Identification of two amino acid residues in the ε subunit that promote mammalian muscle acetylcholine receptor assembly in COS cells. *Neuron*, **6**, 879–887.

Hackam,A.S., Wang,T., Guggino,W.B. and Cutting,G.R. (1997) The N-terminal domain of human GABA receptor r1 subunits contains signals for homo-oligomeric and hetero-oligomeric interaction. *J. Biol. Chem.*, **272**, 13750–13757.

Hall,Z.W. (1992) Recognition domains in assembly of oligomeric membrane proteins. *Trends Cell Biol*., **2**, 66–68.
Hall,Z.W. and Sanes,J.R. (1993) Synaptic structure and development: the neuromuscular junction. *Cell*, **72**, 99–121.
Hebert,D.N., Foellmer,B. and Helenius,A. (1995) Glucose trimming and reglucosylation determine glycoprotein association with calnexin in the endoplasmic reticulum. *Cell*, **81**, 425–433.
Hoch,W., Betz,H. and Becker,C.M. (1989) Primary cultures of mouse spinal cord express the neonatal isoform of the inhibitory glycine receptor. *Neuron*, **3**, 339–348.
Kirsch,J. and Betz,H. (1995) The postsynaptic localization of the glycine receptor-associated protein gephyrin is regulated by the cytoskeleton. *J. Neurosci*., **15**, 4148–4156.
Kirsch,J., Kuhse,K. and Betz,H. (1995) Targeting of glycine receptor subunits to gephyrin-rich domains in transfected human embryonic kidney cells. *Mol. Cell. Neurosci*., **6**, 450–461.
Kreienkamp,H.J., Maeda,R.K., Sine,S.M. and Taylor,P. (1995) Intersubunit contacts governing assembly of the mammalian nicotinic acetylcholine receptor. *Neuron*, **14**, 635–644.
Kuhse,J., Schmieden,V. and Betz,H. (1990a) A single amino acid exchange alters the pharmacology of neonatal rat glycine receptor subunit. *Neuron*, **5**, 867–873.
Kuhse,J., Schmieden,V. and Betz,H. (1990b) Identification and functional expression of a novel ligand binding subunit of the inhibitory glycine receptor. *J. Biol. Chem.*, **265**, 22317–22320.
Kuhse,J., Laube,B., Magalei,D. and Betz,H. (1993) Assembly of the inhibitory glycine receptor: identification of amino acid sequence motifs governing subunit stoichiometry. *Neuron*, **11**, 1049–1056.
Kuhse,J., Betz,H. and Kirsch,J. (1995) The inhibitory glycine receptor: architecture, synaptic localization and molecular pathology of a postsynaptic ion-channel complex. *Curr. Opin. Neurobiol*., **5**, 318–323.
Langosch,D., Thomas,L. and Betz,H. (1988) Conserved quaternary structure of ligand-gated ion channels: the postsynaptic glycine receptor is a pentamer. *Proc. Natl Acad. Sci. USA*, **85**, 7394–7398.
Nicke,A., Bäumert,H.G., Rettinger,J., Eichele,A., Lambrecht,G., Mutschler,E. and Schmalzing,G. (1998) $P2X_1$ and $P2X_3$ receptors form sTable trimers: a novel structural motif of ligand-gated ion channels. *EMBO J*., **17**, 3016–3028.
Pfeiffer,F., Graham,D. and Betz,H. (1982) Purification by affinity chromatography of the glycine receptor of rat spinal cord. *J. Biol. Chem*., **257**, 9389–9393.
Pfeiffer,F., Simler,R., Grenningloh,G. and Betz,H. (1984) Monoclonal antibodies and peptide mapping reveal structural similarities between the subunits of the glycine receptor of rat spinal cord. *Proc. Natl Acad. Sci. USA*, **81**, 7224–7227.
Rickert,K.W. and Imperiali,B. (1995) Analysis of the conserved glycosylation site in the nicotinic acetylcholine receptor: potential roles in complex assembly. *Chem. Biol.*, **2**, 751–759.
Saedi,M.S., Conroy,W.G. and Lindstrom,J. (1991) Assembly of *Torpedo* acetylcholine receptor in *Xenopus* oocytes. *J. Cell Biol*., **112**, 1007–1015.
Schägger,H. and von Jagow,G. (1991) Blue native electrophoresis for isolation of membrane protein complexes in enzymatically active form. *Anal. Biochem*., **199**, 223–231.
Schägger,H., Craner,W.A. and von Jagow,G. (1994) Analysis of molecular masses and oligomeric states of protein complexes by blue native electrophoresis and isolation of membrane protein complexes by two-dimensional native electrophoresis. *Anal. Biochem*., **217**, 220–230.
Schmieden,V., Grenningloh,G., Schofield,P.R. and Betz,H. (1989) Functional expression in *Xenopus* oocytes of the strychnine binding 48 kd subunit of the glycine receptor. *EMBO J*., **8**, 695–700.
Schmieden,V., Kuhse,J. and Betz,H. (1992) Agonist pharmacology of neonatal and adult glycine receptor α subunits: identification of amino acid residues involved in taurine activation. *EMBO J*., **11**, 2025–2032.
Schmieden,V., Kuhse,J. and Betz,H. (1993) Mutation of glycine receptor subunits creates β-alanine receptor responsive to GABA. *Science*, **262**, 256–258.
Schmitt,B., Knaus,P., Becker,C.-M. and Betz,H. (1987) The M_r 93000 polypeptide of the postsynaptic glycine receptor complex is a peripheral membrane protein. *Biochemistry*, **26**, 805–811.
Smith,M.M., Lindstrom,J. and Merlie,J.P. (1987) Formation of the α-bungarotoxin binding site and the assembly of the nicotinic acetylcholine receptor subunits occur in the endoplasmic reticulum. *J. Biol. Chem*., **262**, 4367–4376.
Sontheimer,H., Becker,C.-M., Pritchett,D.B., Schofield,P.R., Grenningloh,G., Kettenmann,H., Betz,H. and Seeburg,P.H. (1989) Functional chloride channels by mammalian cell expression of rat glycine receptor subunit. *Neuron*, **2**, 1491–1497.
Sugiyama,N., Boyd,A.E. and Taylor,P. (1996) Anionic residue in the α subunit of the nicotinic acetylcholine receptor contributing to subunit assembly and ligand binding. *J. Biol. Chem*., **271**, 26575–26581.
Takahashi,T., Momiyama,A., Hirai,K., Hishinuma,B. and Akagi,H. (1992) Functional correlation of fetal and adult forms of glycine receptors with developmental changes in inhibitory synaptic receptor channels. *Neuron*, **9**, 1155–1161.
Thompson,J.A., Lau,A.L. and Cunningham,D.D. (1987) Selective radiolabeling of cell surface proteins to a high specific activity. *Biochemistry*, **26**, 743–750.
Tsigelny,I., Sugiyama,N., Sine,S.M. and Taylor,P. (1997) A model of the nicotinic receptor extracellular domain based on sequence identity and residue location. *Biophys. J*., **73**, 52–66.
Verall,S. and Hall,Z.W. (1992) The N-terminal domains of acetylcholine receptor subunits contain recognition signals for the initial steps of receptor assembly. *Cell*, **68**, 23–31.
Yu,X.M. and Hall,Z.W. (1991) Extracellular domains mediating ε subunit interactions of muscle acetylcholine receptor. *Nature*, **352**, 64–67.

Received May 4, 1999; revised and accepted July 6, 1999